Synthesis and characterization of castor oil-derived oxidation-responsive amphiphilic block copolymers: poly(ethylene glycol)-*b*-poly(11-((2-hydroxyethyl)thio)undecanoate).

Carmen Valverde, Gerard Lligadas, Juan C. Ronda, Marina Galià, Virginia Cádiz.
Departament de Química Analítica i Química Orgànica. Universitat Rovira i Virgili. Campus Sescelades Marcel.lí Domingo 1. 43007 Tarragona. Spain.
Juan Carlos Ronda (E-mail: *juancarlos.ronda@urv.cat*)

ABSTRACT

The synthesis of oxidation-responsive biodegradable amphiphilic block copolymers by *Candida Antarctica Lipase B* (CALB)-catalyzed self-polycondensation of 11-((2-hydroxyethyl)-thio)undecanoic acid (TEHA) initiated by methoxy polyethyleneglycol (mPEG-OH) of different molecular weights has been described. SEC and mono and bidimensional NMR have been used to confirm the molecular weight and structure of the polymers and copolymers. DSC and TGA have been employed to characterize their thermal properties. The oxidation behaviour in front of H_2O_2 as well as the structure of the oxidized products has been established using NMR, FTIR and Raman spectroscopies. The different block copolymers could self-assemble to form nanosized micelles in aqueous solution with low critical micelle concentration (CMC), showing potential application as dual responsive systems in drug delivery. Micellar characteristics were investigated by dynamic light scattering (DLS) and transmission electron microscopy (TEM). These micelles are prone to undergo a H_2O_2-triggered disassembly due to the oxidizable thioether groups in the hydrophobic core. Nile Red was used as model for hydrophobic drugs to test the oxidative triggered release of a copolymer, which showed progressive release in few hours upon the addition of H_2O_2.

KEYWORDS: sulfur-containing polyester, amphiphilic polymer, renewable resource, enzymatic polycondensation, oxidation-responsive, drug delivery.

1. INTRODUCTION

The future success of sustainable polymers, materials derived from renewable feedstocks that are safe in both, production and use, is unquestionable [1]. Nowadays, the interest in polymers from renewable resources has been witnessing an incessant growth in both academic and industrial communities [2,3,4]. Nature provides a wide range of substances such as vegetable oils that can be used as monomers directly or after derivatization. Castor oil is one of the most valuable choices. Their high versatility and exclusion of alimentary sector convert this material in a good candidate to explore new routes to obtain biopolymers. 10-Undecenoic acid [5] and n-heptanal are available from the pyrolysis of castor oil, and they are key substrates in polymer chemistry for the synthesis of precursors for the preparation of sustainable materials. Our group has studied the use of both precursors to the synthesis of functionalized polyesters from sulfur-containing specialty monomers [6-10].

Currently, many research efforts have been directed toward exploiting the special high-performance characteristics of polymers with sulfur in the backbone [11]. Sulfur-containing polymers fall under various classes and cover an extremely broad property range. The impetus to their development resulted from the unique properties and success in their applications, depending upon the type of linkage introduced: thioester [12], thioamide [13], thiourea [14] and thiocarbonate [15,16]. Thus, in the last years sulfur-containing polymers represent an attractive tool for the next generation of functional materials. Also, very recently it has been reported that sulfur-containing polymers, poly(ionic liquid)s and their combinations are emerging macromolecules with unique properties and applications [17].

In recent years, stimuli-responsive polymeric materials have been widely used in biomedical fields. The development of biocompatible and multifunctional polymers with controllable degradation able to respond to physiological and intramolecular stimuli is an area of a great interest. Recent advances and challenges in the developments towards applications of stimuli-responsive polymeric materials that are self-assembled from nanostructured building blocks, are reported. [18,19].

Stimuli-responsive polymers-based anticancer drug delivery systems (DDSs) have shown great advantages for the spatio temporal controllable release of payloads upon the endogenous or exogenous stimulus [20-22]. Recently, reactive oxygen species (ROS) responsive DDSs have been widely studied to deliver and release therapeutic drugs or genes in cancer cells due to the abundant ROS in cancerous cells [23,24]. Many chemical moieties including thioketal, thioether, selenide, and arylboronic ester are found to be ROS-responsive [25-27].

Among the various oxidation-responsive polymers, thioether containing polymers have attracted great interest due to their potential applications in biomedical fields [28-31]. Hydrophobic thioether could be oxidized by ROS to hydrophilic sulfoxide and/or sulfone; this hydrophobic−hydrophilic transition is crucial for disintegration of polythioether-based DDS and could be used for releasing encapsulated bioactive compounds or for uncovering groups capable of specific interactions with cells [32] of anticancer drugs [33-35].

By self-assembly or co-assembly of amphiphilic block copolymers nanosized micelles with a core-shell architecture in a selective solvent have been prepared. They have attracted increasing interest as carriers of biologically active substances (low-molecular-weight drugs, enzymes, DNA, and RNA), antifouling surfaces, biosensors, and so on [36-38]. The hydrophobic core serves as a natural carrier environment for hydrophobic drugs, and the hydrophilic shell stabilizes the particles in aqueous solution [39].

The requirements for biomedical applications favour nanostructures based on assembled amphiphilic macromolecules comprising functional blocks of biological origin and/or biocompatible synthetic polymers. In this respect, the most preferred systems are those composed of polymers approved by the Food and Drug Administration (FDA) for biomedical applications in humans as is the case of polyethyleneglycol (PEG) derivatives [40].

Among the variety of copolymer architectures studied for preparing micellar nanocarriers, the systems based on linear di- or triblock copolymers dominate over others known from the scientific literature [41,42].

In this work, we report the synthesis of oxidation-responsive biodegradable amphiphilic block copolymers by *Candida Antarctica Lipase B* (CALB)-catalyzed self-polycondensation of 11-((2-

hydroxyethyl)thio)undecanoic acid (TEHA) initiated by methoxy polyethyleneglycol (mPEG) of different molecular weights. The hydroxyl thiopolyester (PTEHA) was also synthesized using the same procedure using CALB as catalyst thus avoiding metallic catalysts. TEHA was prepared from the renewable precursor 10-undecenoic acid by thiolene addition of mercaptoethanol under mild conditions. The oxidation behaviour of the PTEHA homopolymer and the mPEG-*b*-PTEHA copolymers with H_2O_2 was studied.

The self-assembly and micellar behaviour of these amphiphilic structures, their ability to disassemble upon addition of H_2O_2 and its potential as a new type of oxidation-responsive polymeric materials against hydrophobic drugs was studied.

2. EXPERIMENTAL

2.1. Synthesis of polymers (Scheme 1)

2.1.1. Homopolymerization of 11-((2-hydroxyethyl)thio)undecanoic acid. Synthesis of PTEHA

In a 25 mL Schlenk flask 1,2 g (4.57 mmol) of 11-((2-hydroxyethyl)thio)undecanoic acid (TEHA) was dissolved in 11.4 mL of dry diphenylether (DPE, 2.5M). Next, 0.12 g (10 % (w/w)) of CALB were added and the mixture was heated with stirring at 90 °C for 1h at atmospheric pressure and under vacuum (0.02 mmHg) for 24h. The polymerization mixture was dissolved in chloroform (10 mL) and CALB beads were removed by filtration and rinsed with some free neat solvent. Chloroform was removed under reduced pressure and the polymer was dissolved in THF and precipitated twice into cold diethylether (200 mL). In this way, a white polymer with Mn 7400 g/mol and $Đ$ 1.6 by SEC and Mn 3200 g/mol by ^{1}H NMR, was obtained in 93 % yield.

^{1}H NRM ($CDCl_3$/TMS, δ ppm): 4,21 (t, 2H, CH_2OOC), 3.70 (t, 2H, $C\underline{H}_2$-OH, end group), 2,73 (t, 2H, S-$C\underline{H}_2$-CH_2-O), 2.55 (t, 2H, ($C\underline{H}_2$-S-CH_2-CH_2-O), 2.52 (t, 2H, ($C\underline{H}_2$-S-CH_2-CH_2-OH, end group) 2.31 (t, 2H, CH_2-COO), 1.64-1.27 (m, 16H, $(CH_2)_8$).

^{13}C NMR ($CDCl_3$, δ ppm): 173.80 (COO), 63.46 ($\underline{C}H_2OCO$), 60.05 (CH_2-OH, end group), 34.34 ($\underline{C}H_2$-COO), 32.47 ($\underline{C}H_2$-S-CH_2-CH_2-O), 30.58 (CH_2-S-$\underline{C}H_2$-CH_2-O), 29.90-28.45 ($(CH_2)_8$), 25.02 ($\underline{C}H_2$-CH_2-CO).

2.1.2 Polymerization of TEHA in presence of mPEG-OH - Synthesis of $mPEG_n$-b-$PTEHA_m$

In a typical procedure, monomethoxy poly(ethylene glycol) MW 550 ($mPEG_{12}OH$) (0.21 g, 0.38 mmol or 0.10 g, 0.02 mmol) or MW 2000 ($mPEG_{45}OH$) (0.76 g, 0.38 mmol or 0.38 g, 0.02mmol), TEHA (1.0 g, 3.81 mmol), and toluene (200 wt % vs. total substrates) were placed into a Schleck flask. The feed molar ratios of $mPEG_nOH$/TEHA were 1:10 and 1:20. CALB (10 wt % vs. total substrates) was transferred into the flask and the suspension stirred and heated at 90 ^oC for 48 h. Chloroform (10 mL) was added to the polymerization mixture and the enzyme was removed by filtration. The resulting solution was washed with water and precipitated twice in cold hexane (100 mL) and the polymer collected by filtration, rinsed with hexane and dried under vacuum.

^1H NRM ($CDCl_3$/TMS, δ ppm): 4.30 (t, 2H, O-$CH_2C\underline{H}_2$-OCO), 4.21 (t, 2H, O-$C\underline{H}_2CH_2$-S), 3.72 (t, 4H, HO-$C\underline{H}_2$ and -$OC\underline{H}_2CH_2OCO$), 3.65 (s, 4H, (O-$C\underline{H}_2$-$C\underline{H}_2$-)$_n$, 3.56 (t, 2H, CH_3-O-$C\underline{H}_2$), 3.38 (s, 3H, CH_3-O), 2.73 (t, 2H, O-CH_2-$C\underline{H}_2$-S), 2.55 (t, 2H, ($C\underline{H}_2$-S-CH_2-CH_2-O), 2.49 (t, 2H, $C\underline{H}_2$-S-CH_2-CH_2OH, end group), 2.31 (t, 2H, CH_2-COO), 2.20 to 1.80 (broad s, 1H, OH), 1.64-1.27 (m, 16H, $(CH_2)_{16}$).

^{13}C NMR ($CDCl_3$, δ ppm): 177.9 ($OCH_2CH_2O\underline{C}O$), 173.8 ($SCH_2CH_2O\underline{C}O$), 71.9 (CH_3-O-$\underline{C}H_2$-CH_2O), 70.6 (O-$\underline{C}H_2$-$\underline{C}H_2$-O), 69.1 (O-$\underline{C}H_2$-CH_2-OCO), 64.0 (O-CH_2-$\underline{C}H_2$-OCO), 63.4 (S-CH_2-$\underline{C}H_2$-OCO), 60.2 (CH_2-OH), 59.0 (CH_3-O), 35.1 (OOC-$\underline{C}H_2$-$(CH_2)_8$-CH_2-S-CH_2-CH_2OH, end group), 34.3 (OOC-$\underline{C}H_2$), 32.5 ($\underline{C}H_2$-S-CH_2-CH_2-OCO), 31.2 ($\underline{C}H_2$-S-CH_2-CH_2OH, end group), 30.9 (S-$\underline{C}H_2$-CH_2-OCO), 30.6-28.9 $(CH_2)_6$.

2.2. Polymer oxidations.

All oxidation experiments were performed following a protocol adapted from reported procedures. [30, 43, 44] About 50 mg of polymer (PTEHA or $mPEG_{12}$-*b*-$PTEHA_9$) were suspended in 1 mL of deionized water. Next, 1 mL of 2 % (w/v) H_2O_2 and 1mL of toluene were added. Finally, 5 mg of phosphomolibdic acid and one drop of Aliquad 336 were also added. The heterogeneous mixture was stirred vigorously at 200 rpm and at 25 ^oC. After 24 h the sample was withdrawn and 1 mL of sodium sulphite (1 M) was added to reduce unreacted H_2O_2. The solution mixture was extracted with chloroform, washed twice with water and, after drying with anhydrous magnesium sulphate, concentrated to about 5 mL. Polymers were isolated by precipitation in cold diethyl ether. The same procedure was also tested at 50 °C for 24h in the

case of PTEHA. The resulting oxidized products were analysed by ^{1}H NMR, ^{13}C NMR and FTIR-ATR, and in some cases by Raman spectroscopy.

2.2.1 Oxidation of PTEHA. Synthesis of (O)PTEHA and (O_2)PTEHA

^{1}H NMR ($CDCl_3$/TMS, δ ppm): 4.55-4.45 (m, 2H, O-C<u>H</u>$_2$-CH_2-SO-), 4.51 (t, 2H, O-C<u>H</u>$_2$-CH_2-SO_2), 4,10 (m, 2H, HOC<u>H</u>$_2$-CH_2-SO_2), 3.27 (t, 2H, OCH_2-C<u>H</u>$_2$-SO_2), 3.19 (m, 2H, $HOCH_2$-C<u>H</u>$_2$ -SO_2), 3.07 (m, 2H, $HOCH_2$-CH_2-SO_2-C<u>H</u>$_2$), 3.00 (m, 2H, -OCH_2-CH_2-SO_2-C<u>H</u>$_2$), 2.95 (m, 2H, -OCH_2-C<u>H</u>$_2$-SO), 2.72 (m, 2H, OCH_2-CH_2-SO-C<u>H</u>$_2$), 2.32 (t, 2H, CH_2-COO), 1.84-1.28 (m, 16H, $(CH_2)_8$).

^{13}C NMR ($CDCl_3$, δ ppm): 173.8 (OOC in SO units), 173.2 (OOC in SO_2 units), 57.9 (O-<u>C</u>H_2-CH_2-SO_2), 57.5 (O-<u>C</u>H_2-CH_2-SO), 56.8 (HO-<u>C</u>H_2-CH_2-SO_2), 55.4 (HO-CH_2-CH_2-SO_2-<u>C</u>H_2), 54.8 (HO-CH_2-<u>C</u>H_2-SO_2), 54.6 (O-CH_2-CH_2-SO_2-<u>C</u>H_2), 53.2 (O-CH_2-CH_2-SO-<u>C</u>H_2), 52.1 (O-CH_2-<u>C</u>H_2-SO_2), 51.9 (O-CH_2-<u>C</u>H_2-SO), 34.6 (<u>C</u>H_2-COO), 30.1-22.4 ($(CH_2)_8$).

FTIR (cm^{-1}): 1690 (CO), 1265 and 1123 (SO_2), 1020 (SO).

Raman (cm^{-1}): 1124 (SO_2), 1025 (SO).

2.2.2. Oxidation of $mPEG_n$-*b*-$PTEHA_m$. *Syhthesis of* $mPEG_n$-*b*-(O)$PTEHA_m$ *and* $mPEG_n$-*b*-(O_2)$PTEHA_m$

^{1}H NMR ($CDCl_3$/TMS, δ ppm): 4.55-4.45 (m, 4H, O-C<u>H</u>$_2$-CH_2-SO and O-C<u>H</u>$_2$-CH_2-SO_2), 4.28 (t, 2H, O-CH_2-C<u>H</u>$_2$-OCO), 4.20 (m, 2H, HO-C<u>H</u>$_2$-CH_2-SO_2), 3.74 (t, 2H, O-C<u>H</u>$_2$-CH_2-OCO), 3.65 (s, 4H, (O-C<u>H</u>$_2$-C<u>H</u>$_2$-)$_n$, 3.52 (t, 2H, CH_3-O-C<u>H</u>$_2$), 3.41 (m, 2H, O-CH_2-C<u>H</u>$_2$-SO_2), 3.39 (s, 3H, C<u>H</u>$_3$-O), 3.28 (m, HO-CH_2-C<u>H</u>$_2$-SO_2), 3.00-2.70 (m, 6H, O-CH_2-CH_2-SO_2-C<u>H</u>$_2$, O-CH_2-C<u>H</u>$_2$-SO_2-CH_2 and C<u>H</u>$_2$-O-CH_2-CH_2-SO),2.33 (t, 2H, CH_2-COO), 1.84-1.28 (m, 18H, $(CH_2)_8$).

^{13}C NMR ($CDCl_3$, δ ppm): 173.4 (COO), 72.0 (CH_3-O-<u>C</u>H_2-CH_2-O), 70.6 (O-<u>C</u>H_2-<u>C</u>H_2-O), 69.2 (O-<u>C</u>H_2-CH_2-OCO), 64.1 (O-CH_2-<u>C</u>H_2-OCO), 59.0 (CH_3-O), 57.8 (O-<u>C</u>H_2-CH_2-SO_2), 54.3 (O-CH_2-CH_2-SO_2-<u>C</u>H_2), 52.4 (O-CH_2-<u>C</u>H_2-SO_2), 34.7 (<u>C</u>H_2-COO), 30.1-22.4 ($(CH_2)_8$).

FTIR (cm^{-1}): 1696 (CO), 1260 and 1128 (SO_2), 1026 (SO).

2.3. Copolymers self-assembly behavior.

2.3.1. Micelles preparation and characterization.

Block copolymer micelles were prepared by the co-solvent evaporation nano-precipitation method. Samples of $mPEG_n$-*b*-$PTEHA_m$ were directly dissolved in HPLC grade THF (1 mL/5 mg) and added dropwise to deionized water at room temperature with stirring (800 rpm). THF was gradually evaporated by bubbling argon during 60 min and the resulting micellar solution was filtered through a membrane syringe filter (0.20 μm) and diluted with HPLC water to obtain a 1.0 mg/mL concentration. Average size, size distribution and Z-average of micelles were determined by Dynamic Light Scattering (DLS) at 25° C. The Stokes-Einstein equation was used by the instrument to calculate Z-average size. Size and morphology of the polymeric micelles were analysed with a JEOL-JEM 1011 transmission electron microscopy (TEM) in drying and negative stain mode. Typically, a drop of polymer solution (25-50 μg/ml) was dropped onto a 200-mesh Formvar carbon-coated cooper grid (TED-PLLA Inc.) and dried at ambient conditions for at least for 12 h. In the stain mode, a solution of 2% phosphotungstic acid (PTA) was added to the droplet and the excess solution was removed by wicking with filter paper. Samples were imaged in bright field at tension of 80 KV using an ITEM imaging software at magnifications 40000 to 500000.

2.3.2. Critical micelle concentration (CMC) measurements.

The critical micelle concentration of copolymers was determined by the pyrene 1:3 ratio method [45]. Typically, stock mater solution of fluorescent probe ($6.0 \cdot 10^{-7}$ M) in THF was prepared and pre-calculated volumes were transferred to vials followed by argon flow evaporation. Different concentrations (from 1.0 $mg.mL^{-1}$ to $1 \cdot 10^{-6}$ $mg \cdot mL^{-1}$) of copolymer solutions in water were added and the mixture stirred overnight protected from light. Samples were excited at 335 nm, and the emission spectra were recorded from 350 to 500 nm at room temperature. The intensity values of fluorescence emission, I_{372} and I_{382} at 372 nm and 382 nm, respectively, were used from the subsequent calculations. The CMC was determined from the plots of the I_{382}/I_{372} ratio versus the logarithm of the polymer concentration using the intersection of the linear regression lines as the CMC values. All solutions were filtered through filters of 0.20 μm pore size before DSL measurements that were made by triplicate.

2.4. Nile Red encapsulation and H_2O_2-triggered release of $mPEG_{12}$-*b*-$PTEHA_{15}$ copolymer .

Nile Red-loaded micelles were prepared by the film hydration method [46]. 50 mg of the $mPEG_{12}$-*b*-$PTEHA_{15}$ and 0.25 mg of Nile Red were co-dissolved in 2.5 mL of THF. Then, the solvent was removed using a rotary evaporator at room temperature to form a solid thin film. Subsequently, the solid thin film was treated with 10 mL of deionized water in bath at 60 ^{o}C for 5 min and vortexed for two additional min. After cooling to room temperature, the solution was transferred into a 25 mL volumetric flask and diluted with deionized water to a final polymer concentration of 2 mg/mL which was filtered through 0.20 μm membrane to remove non-encapsulated Nile Red and stored at 4 ^{o}C as stock solution of Nile Red-loaded micelles.

The Nile Red release was performed by mixing 2 mL of the stock solution with 2 mL of H_2O_2 solutions of different concentration and incubated at 37 ^{o}C for one hour. The fluorescence spectra with an excitation wavelength of 557 nm, were recorded at different time intervals. The intensity value of fluorescence emission at 637 nm was measured and related with the initial fluorescence intensity (100 % intensity).

2.5. Instrumentation

^{1}H (400 MHz) and ^{13}C (100.5 MHz) NMR spectra were recorded using a Varian Gemini 400 spectrometer. Spectra were recorded at room temperature using 10-15 mg (^{1}H) or 30-40mg (^{13}C NMR) of sample in $CDCl_3$ as solvent and TMS (^{1}H NMR) as internal standard. In ^{13}C NMR the central peak of the deuterated solvent was taken as reference and the chemical shifts given in ppm from TMS using appropriate shifts conversions. ESI-TOF measurements were carried out using an Agilent 1200 liquid chromatography coupled to 6210 Time of Flight (TOF) mass spectrometer from Agilent Technologies (Waldbronn, Germany) with an ESI interface. The FTIR spectra were recorded on a JASCO 680 FTIR spectrophotometer with a resolution of 4 cm^{-1} in the transmittance mode. An attenuated total reflection (ATR) accessory and a diamond crystal (Golden Gate single-reflection diamond ATR, Specac, Teknokroma) was used. Raman spectra were recorded at room temperature on a Renishaw FT-IR Raman spectrophotometer with a Leica DM 2500 confocal microscope with FT-IR IluminatIR II system and using a Streamline Raman Imaging software.

Calorimetric studies were carried out on a Mettler DSC3+ Star system thermal analyzers using N_2 as a purge gas (100 ml/min) at scanning rate of 10 °C/min in the -80 to 250°C temperature range. Calibration was made using an indium standard (heat flow calibration) and an indium-lead-zinc standard (temperature calibration). Size exclusion chromatography (SEC) analysis in THF was carried out with an Agilent 1200 series system equipped with three serial columns (PLgel 3µm MIXED-E, PLgel 5µm MIXED-D and PLgel 20m MIXED-A from Polymer Laboratories) and an Agilent 1100 series refractive-index detector working at room temperature at a flow rate of 1.0 mL/min. Size exclusion chromatography (SEC) analysis in THF was carried out with an Agilent 1200 series system equipped with three serial columns (PLgel 3µm MIXED-E, PLgel 5µm MIXED-D and PLgel 5µm MIXED-C from Polymer Laboratories) and an Agilent 1200S refractive-index detector working at 40 °C at a flow rate of 1.0 mL/min. In both cases calibration curves for SEC analysis were obtained with polystyrene standards. Dynamic Light Scattering measurements were performed on a Malvern NanoZS instrument, equipped with an avalanche photodiode detector and a solid state laser He-Ne laser with output power was 4 mW at λ = 632.8 nm) at a scattering angle of 90°. Fluorescence spectra were obtained on an RF-5301 PC Shimatzu fluorescence spectrometer with RFPC software with emission using excitation slit widths of 5 nm. Transmission electron microscopy (TEM) observations were carried out on a JEOL 1011 high-resolution transmission electron microscope at an accelerating voltage of 80 KV. Samples were imaged in bright field at tension of 80 Kv using an ITEM imaging software.

3. RESULTS AND DISCUSSION

Recently, our group reported the preparation of micelles from PEG-modified poly(10,11-dihydroxyundecanoic acid) amphiphilic copolymers [47]. We extend this methodology to the preparation of oxidation-responsive polymeric materials with β-thioether ester groups.

Candida antarctica lipase B (CALB) is by far the most studied enzymatic catalyst as it is commercially available in a supported form as Novozym 435, offering additional advantages as easy manipulation, easy removal from the polymerization mixture and robust nature. The polycondensation of monomers containing both hydroxyl and carboxyl groups in the same structure has been described with CALB [48, 49]. The efficiency of enzymatic catalysts can be

affected by process parameters such as polymerization temperature, polymerization technique (solution or solvent-free) as well as water removal methods (e.g. application of vacuum, water absorption in molecular sieves, azeotropic distillation). Thus, after some preliminary essays, polymerization conditions were fixed using 10% (w/w) of CALB at 90º C in DPE for 24h in the case of the homopolymers and in toluene for 48 h in the case of copolymers with mPEG-OH.

3.1. Synthesis of poly (11-(2-hydroxyethyl)thioundecanoic acid) (PTEHA)

The synthesis of TEHA, a thioether-containing ω-hydroxyacid (Scheme 1a, SI.1) was carried out by thiol-ene coupling of 2-mercaptoethanol and 10-undecenoic acid initiated by 2,2-dimethoxy-2-phenylacetophenone (DMPA) [50]. Next, this AB monomer, with both hydroxyl and carboxylic functionalities, was polymerized by self-condensation in DPE at 90º C for 24 h to produce PTEHA (Scheme 1a), in 93 % yield with Mn 7400 g/mol and *Đ* 1.6 determined by SEC. (SI.2.1).

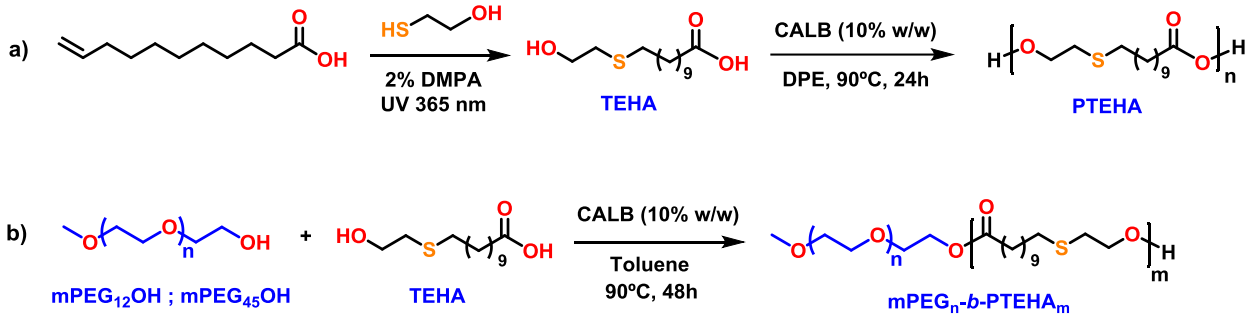

Scheme 1. a) Synthesis of TEHA and PTEHA; **b)** Polymerization of TEHA in presence of mPEG-OH

PTEHA structure was confirmed by ^{1}H and ^{13}C NMR and heteronuclear single quantum correlation (HSQC) spectrum (Figures SI.3 and SI.4). ^{1}H NMR spectrum collected in Figure 1a, shows a triplet at 4.21 ppm characteristic of a methylene linked to -OCO in the repeating unit. Moreover, a triplet with small intensity at 3.70 ppm corresponding to CH_2-OH end groups could be observed. From the relative intensity of both signals, Mn was estimated about 3200 g/mol, being this value significantly lower than the one determined by SEC (7400 g/mol) probably due to the differences in hydrodynamic volume with PS standards used. The polydispersity observed for this homopolymer is quite narrow (*Đ* 1.6) which can be related with fractionation processes during the work-up.

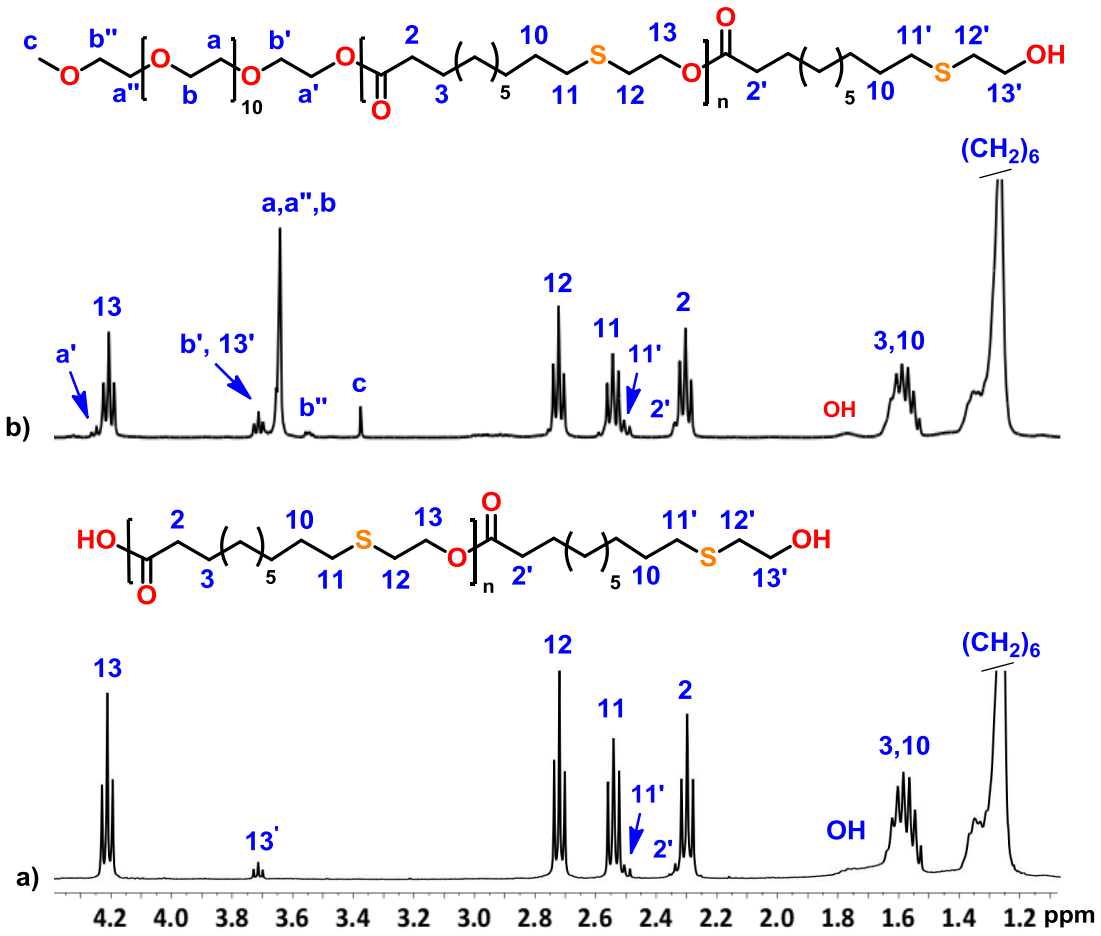

Fig. 1. ^{1}H NMR spectra of **a)** PTEHA and **b)** Polymer mPEG$_{12}$-*b*-PTEHA$_{9}$

PTEHA thermal characterization by DSC (Figure SI.5, Table 2) evidences its high crystalline structure with a narrow melting endotherm at 67º C. By comparing to poly(11-hydroxyundecanoic acid) with similar molecular weight (by ^{1}H NMR) [51] which presents a melting point of 73º C, it can be inferred that the sulphur in the repeating unit disturbs somewhat chain packaging. Moreover, the presence of a significant exotherm in the cooling scan and an endotherm in the second heating scan indicate its ability to reorganize and crystallize.

3.2. Polymerization of TEHA in presence of mPEG-OH and TEHA. Synthesis of mPEG$_n$-b-PTEHA$_m$.

The synthesis of copolymers was more challenging. In the literature, amphiphilic copolymers were mostly prepared by CALB catalyzed chemical modification of the corresponding methyl or

vinyl esters through a transesterification reaction, but some few examples using free carboxylic acids also do exist [52, 53]. The good results obtained in the homopolymerization of TEHA led us to test CALB in different solvents and temperatures. The use of toluene at 90 °C for 48 h led to better results in terms of conversion and copolymer composition.

Two commercial monomethylated mPEG-OH with Mn 550 and 2000 g/mol were selected as hydrophilic macromonomers (Scheme 1b). Their formula weight corresponds to 12 and 45 ethylenoxy repeating units, and were named as $mPEG_{12}OH$ and $mPEG_{45}OH$. For each mPEG-OH two different feed molar ratios $mPEG_nOH$/TEHA were used: 1:10 and 1:20. Procedures are described in SI.2.2 and results are summarized in Table 1.

According to the ^1H and ^{13}C NMR spectra of the crude reaction mixture, high $mPEG_n$-OH conversion was achieved but TEHA incorporation was lower than those in the feed was. Percentage of chains initiated by mPEG was considerable high (Figures SI.6 and SI.7). By repeated precipitations in hexane and washings with warm water, the remaining unreacted TEHA and traces of mPEG-OH could easily be removed (confirmed by ^{13}C NMR spectroscopy, Figures SI.8 and SI.9).

Table 1. Composition and molecular weight of $mPEG_n$-*b*-$PTEHA_m$ polymers obtained after 48h with CALB in toluene at 90 °C.

	mPEG-OH/TEHA molar ratio		**Molecular weight**		
Block copolymer	Feed	^1H NMR[(a)]	$Mn^{(a)}$ (g/mol)	$Mn^{(b)}$ (g/mol)	$Mw/Mn^{(b)}$
$mPEG_{12}$-*b*-$PTEHA_9$	1:10	1:09	2750	2600	1.9
$mPEG_{12}$-*b*-$PTEHA_{15}$	1:20	1:15	4220	3500	1.8
$mPEG_{45}$-*b*-$PTEHA_9$	1:10	1:09	4200	2100	1.8
$mPEG_{45}$-*b*-$PTEHA_{15}$	1:20	1:15	5660	5400	1.6

a) Determined by ^1H NMR from signals at 3.38 and 2.35 ppm; b) Determined by SEC in THF.

The copolymer compositions were determined by ^{1}H NMR taking into account the relative intensities of the signals at ca. 2.35 ppm of the α-methylene to ester group (CH_2-COO), and at 3.38 ppm of methyl of $mPEG_n$. Thus, when working with 1:10 feed molar ratio, 90% of the TEHA was incorporated to $mPEG_n$-OH which correspond to polymers with molar composition $mPEG_{12}$-$PTEHA_9$ and $mPEG_{45}$-$PTEHA_9$. In the case of 1:20 molar ratio, only 75% of the TEHA was incorporated to mPEG-OH which correspond to copolymers with molar composition $mPEG_{12}$-*b*-$PTEHA_{15}$ and $mPEG_{45}$-*b*-$PTEHA_{15}$ (Table 1). In Figure 1b the ^{1}H NMR spectrum of $mPEG_{12}$-*b*-$PTEHA_9$ with the corresponding assignments in a representative structure is shown. Molecular weights determined by SEC (Figure SI.10) were in good agreement to those estimated by ^{1}H NMR spectroscopy from end group signals. This behavior is different to the observed in PTEHA homopolymer and indicates a different hydrodynamic behavior due to the presence of the hydrophilic moieties. Besides, owing that fractionation occurs during the purification work up, polydispersity indexes (Đ) are quite narrow (in rang of 1.6-1.9) but in some cases some low molecular weight oligomers were not completely eliminated (Figure SI.10 b) and d)).

3.3 Copolymers thermal characterization

The thermal characteristics of block copolymers were determined by DSC (Figure SI.11) and TGA and are collected in Table 2. DSC analysis show a similar behavior for all copolymers: a single broad exotherm in the first heating, a narrow crystallization endotherm below room temperature in the cooling and a melting exotherm at higher temperature in the second heating scan. No transitions attributable to PEG moieties are observed. Respects to melting temperature endotherms, all of them were lower than the observed for PTEHA homopolymer. Copolymers with $mPEG_{45}$ show lower melting enthalpies owing to their lower percentage of PTEHA moieties.

Referring to thermal stability evaluated by TGA scarce differences between the homopolymer and its corresponding block copolymers in both $T_{5\%}$ and T_{max} were observed. Polymers and copolymers with high percentages of PTEHA present a two steps degradation whereas copolymers in which m-PEG dominates seems to show a single step degradation.

Table 2. Thermal properties of PTEHA and their block copolymers.

Polymer	DSC analysis		TGA analysis	
	Tm [(a)] (°C)	ΔH [(a)] (J/g)	$T_{5\%}$ [(b)] (°C)	T_{max} [(c)] (°C)
PTEHA	67	-170	365	408/479
mPEG$_{12}$-*b*-PTEHA$_9$	50	-80	360	408/454
mPEG$_{12}$-*b*-PTEHA$_{15}$	51	-71	360	409/463
mPEG$_{45}$-*b*-PTEHA$_9$	47	-45	371	417
mPEG$_{45}$-*b*-PTEHA$_{15}$	47	-53	362	409

(a) Melting temperatures (T_m) and enthalpies (ΔH_m) determined by DSC on the second heating scan at heating rates of 10 °C·min^{-1}; (b) Temperature at which 5% weight loss was observed by TGA; (c) Temperature for maximum degradation rate from TGA.

3.4. Oxidation of PTEHA and mPEG$_n$-b-PTEHA$_m$

Effective oxidation of thioether moieties is crucial to induce the hydrophobic to hydrophilic transition into the micellar self assemblings. Thioether undergoes facile oxidation to more hydrophilic sulfoxides or sulfones upon oxidation to H_2O_2 and different methodologies are described [30,44]. Preliminary experiments with H_2O_2 alone, led to a partial oxidation and extensive hydrolysis of polymers. Heteropolyacids have been described to effectively catalyze H_2O_2 oxidation under phase transfer catalysis (PTC) conditions [43]. Thus, a study using phosphomolibdic acid as catalyst and aliquat 336 as phase transfer agent in toluene/2% H_2O_2, with PTEHA was carried out to set the more effective oxidation conditions (Scheme 2).

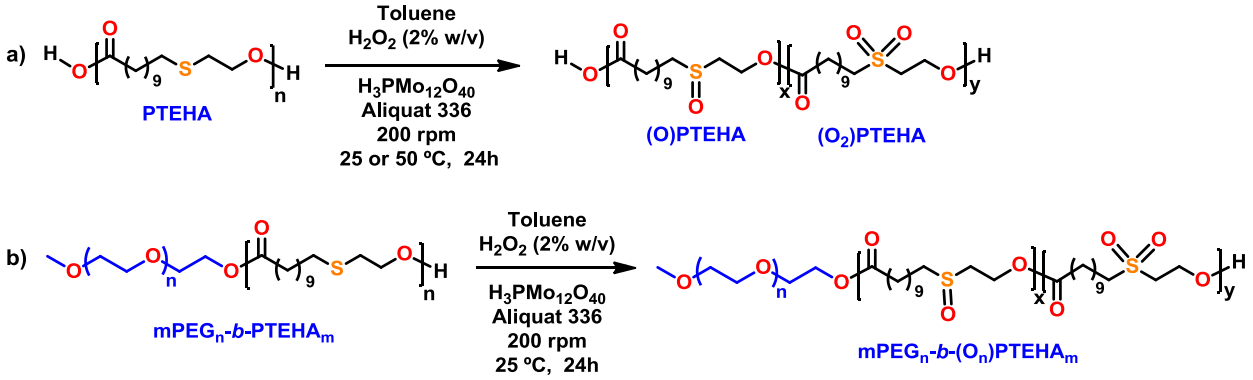

Scheme 2. Oxidation of **a)** PTEHA; **b)** mPEG$_n$-*b*-PTEHA$_m$ with H_2O_2.

Two experiments at temperatures of 25 º C and 50 º C, for 48 h were carried out (SI 3.1). By ^{1}H NMR spectroscopy (Figures 2a and SI 12a) it could be observed that at room temperature complete oxidation takes place giving the expected sulfone ((O$_2$)PTEHA$_m$) and a small percentage of sulfoxide ((O)PTEHA$_m$) moieties. The low intensity of end groups signals indicates that no significant hydrolysis occurs. On the contrary, working at 50 ºC, led to a polymer with the same signals but being the more intense those corresponding to end groups, due to hydrolysis. It must be pointed out that complete structural characterization of these two samples using ^{1}H, ^{13}C NMR spectroscopy including HSQC correlations (Figures SI.12 and SI.13) allowed the unequivocal assignments of sulfoxide and sulfone groups signals in the repeating unit and the sulfone in the end group signals. This characterization was used as model to assign signals in oxidized polymers. In the case of (O$_2$)PTEHA the relative signals intensity indicate than over 90 % of the units have been oxidized to sulfone. The presence of sulfoxide and sulfone moieties was confirmed by Raman and FITR-ATR spectroscopy (figure SI.14) which show the respective characteristic bands of sulfoxide (Raman 1025 cm^{-1} ; FTIR 1020 cm^{-1}) and sulfone (Raman 1124 cm^{-1} ; FTIR 1123 cm^{-1} and 1265 cm^{-1}) being those of sulfone the more intense.

Oxidation with H_2O_2 at room temperature under PTC conditions was applied to mPEG$_n$-*b*-PTEHA$_m$ copolymers (SI 3.2). ^{1}H and ^{13}C NMR spectra of different samples were similar and indicated the presence of a mixture of sulfoxide and sulfone (mPEG$_n$-*b*-(O$_n$)PTEHA$_m$) in comparable percentages (Figures 2b and SI.15). Notably, signals attributed to end groups show a very small intensity indicating no significant hydrolysis occurs.

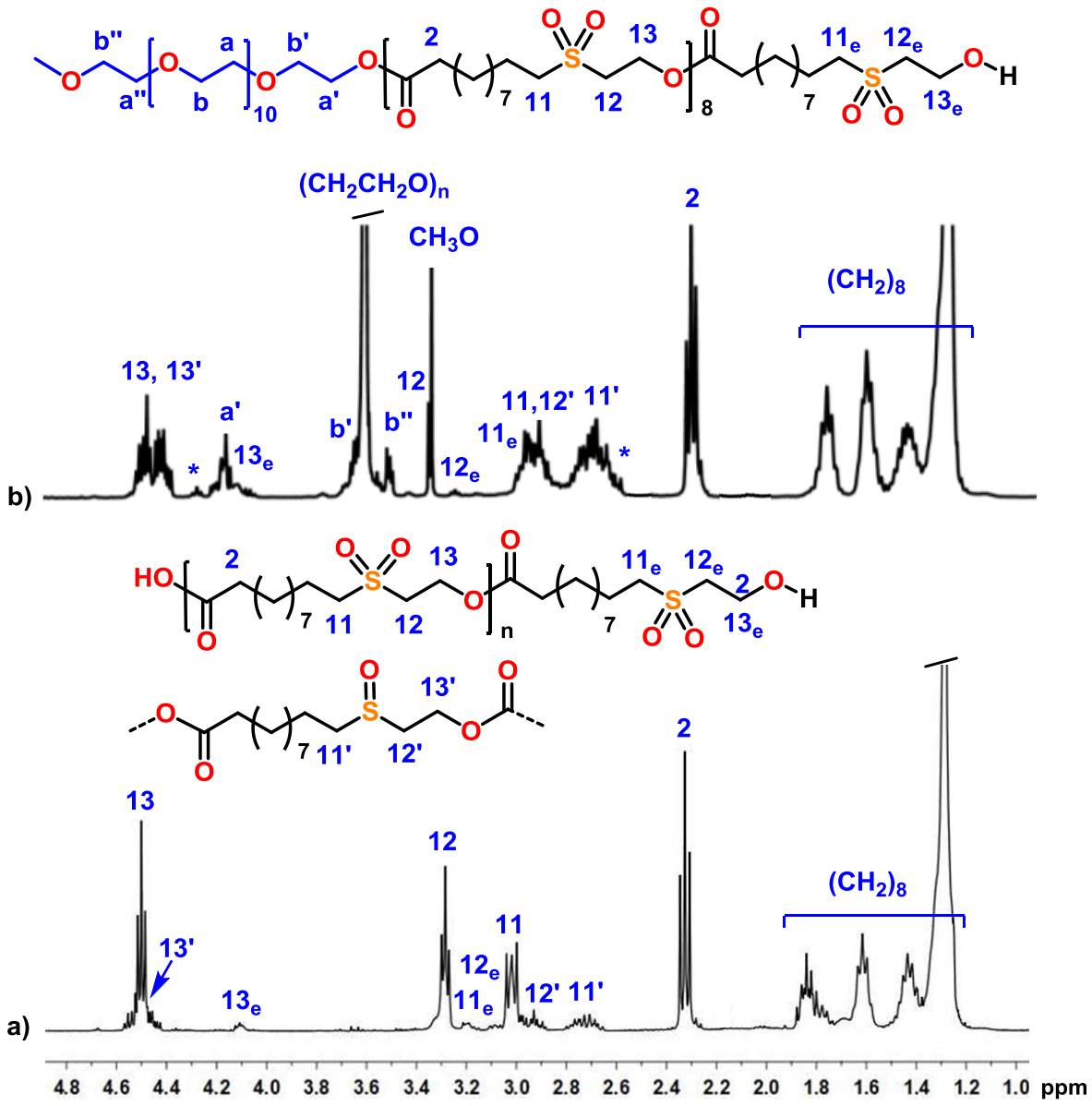

Figure 2. ^{1}H NMR spectra of **a)** (O_2)PTEHA; **b)** mPEG$_{12}$-*b*-(O_n)PTEHA$_9$

FTIR spectrum (Figure SI.16) confirms the presence of sulfoxide (1026 cm^{-1}) and sulfone (1128 cm^{-1} and 1260 cm^{-1}) moieties. Taking into account the relative intensity of the absorptions bands, higher percentages of sulfoxide groups than in PTEHA were detected. This is in agreement to the relatively higher intensity of the sulfoxide signals in ^{1}H NMR spectrum. The lower oxidation degree could be also inferred from the presence of small intensity signals of pristine thioether units (marked with an asterisk in Figures 2b and SI.15).

3.5. Copolymers self-assembly behaviour

All PTEHA-based mPEG block copolymers showed a great ability to self-assemble to form different unimolecular and mainly multimolecular round shaped micelles. The high hydrophobicity of the PTEHA block allows forming a dense core arranging the mPEG hydrophilic block in the shell, thus leading to stable supramolecular micelles. The micellar characteristics of the different copolymers are collected in Table 3 and DLS plots measured at 0.5 mg/mL solution in water are collected in Figure SI. 17.

Table 3. Micellar characteristics of the copolymers $mPEG_n$-*b*-$PTEHA_n$ obtained after 48h with CALB in toluene at 90 °C.

Block copolymer	Micellar characteristics			
	Size[(a)] (nm)	PdI[(a)]	Z_{av}[(a)] (nm)	CMC[(b)](mgL^{-1})
$mPEG_{12}$-*b*-$PTEHA_9$	245±3	0.188±0.01	239±4	0.16
$mPEG_{12}$-*b*-$PTEHA_{15}$	223±9	0.242±0.03	231±1	0.51
$mPEG_{45}$-*b*-$PTEHA_9$	193±2 65±4	0.320±0.02	209±3	0.21
$mPEG_{45}$-*b*-$PTEHA_{15}$	193±7 909±100	0.490±0.01	322±4	0.30

a) Size and PdI (size polydispersity index) of micelles (1mg mL^{-1}) determined by DLS; b) Determined using pyrene as fluorescence probe

Unimolecular micelles (< 20 nm) were not detected by DLS at 0.5 mg/mL concentration. Measurements at lower concentrations (0.01 and 0.05 mg/mL) showed also the formation of multimolecular micelles of similar shape. Amphiphilic copolymer with short PEG chains ($mPEG_{12}$-*b*-$PTHEA_9$ and $mPEG_{12}$-*b*-$PTEHA_{15}$) show a single micellar distribution with size diameter about 230 nm. On the contrary, copolymers with longer PEG chains show a different behaviour with bimodal distributions. $mPEG_{45}$-*b*-$PTEHA_9$ presents mainly micelles with average diameter about 190 nm with a small population of smaller micelles (~ 65 nm). In the case of $mPEG_{45}$-*b*-$PTEHA_{15}$, apart from micelles of 190 nm a high proportion of much larger aggregates

(900±100 nm) were detected. This seems to indicate that the large PEG domains tend to interact leading to molecular clusters under certain conditions.

Delightfully, TEM images under negative stain (PTA) (Figure 3a and Figure SI 18) show nice distributions of unimolecular micelles, with roughly spherical shape, ranging 15-40 nm in all samples. Not multimolecular micelles or micelle aggregates could be observed. This different behaviour has to be attributed to the different conditions during sample preparation. So, according to DLS and TEM results the length of the flexible PEG moiety seems not to be determinant in the particle size but promotes secondary unimolecular micelle aggregation processes in water solution leading to multimolecular assemblies or higher aggregates.

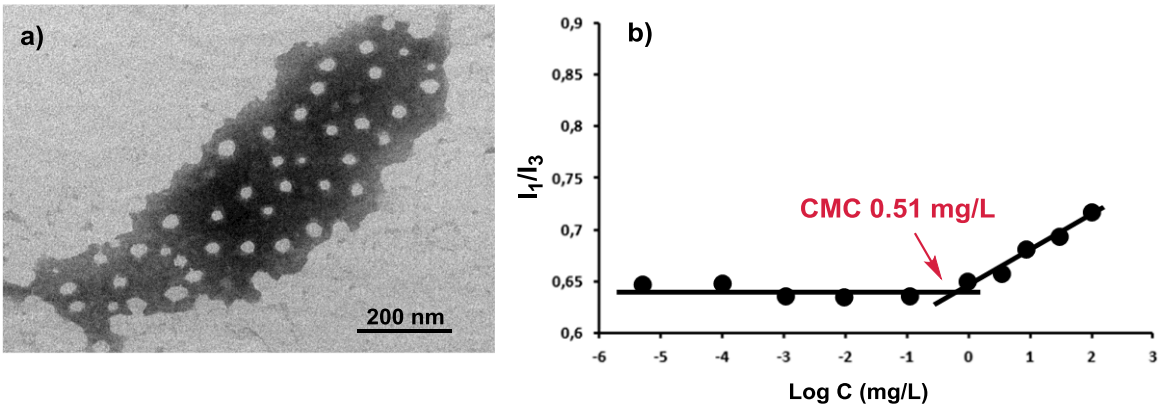

Figure 3. a) TEM images of $mPEG_{12}$-*b*-$PTHEA_9$ micelles obtained in drying mode, b) Calculation of CMC using the I_1/I_3 intensity ratio method based on the fluorescence spectra of pyrene for $mPEG_{12}$-*b*-$PTEHA_{15}$.

The self-assembling of all $mPEG_n$-*b*-$PTEHA_m$ copolymers was confirmed by critical micelle concentration measurements (Table 3, Figure 3b and Figure SI.19) from the I_1/I_3 fluorescence intensity ratio using pyrene [54]. CMC between 0.16 and 0.51 mg/mL were found indicating that at relatively low concentrations in water, unimolecular micelles spontaneously aggregate together forming supramolecular multimolecular micelles that increase the solubility of the fluorescent probe. Increasing the percentage of PTHEA block seems to slightly increase the CMC, but no significant differences between $mPEG_{12}$- and $mPEG_{45}$- were found. Disappointingly, little steep slopes over CMC are obtained with the exception of $mPEG_{12}$-co-

$PTEHA_{15}$, indicating a general low loading capacity of these systems in contrast to the behaviour reported for similar polymers but more polar [30].

3.6. Nile Red encapsulation and H_2O_2-triggered release of $mPEG_{12}$-*b*-$PTEHA_{15}$ copolymer.

$mPEG_{12}$-*b*-$PTEHA_{15}$ was selected to test the oxidative triggered release of hydrophobic drugs, owing its superior loading capacity for pyrene. Nile Red was chosen as model for hydrophobic drugs. To encapsulate the Nile Red into nanoparticles, the film hydration method was used [46], starting from a film formed from a mixture of $mPEG_{12}$-*b*-$PTEHA_{15}$ (50 mg) and Nile Red (25 mg). DLS measurements show that Nile Red encapsulation lead to the formation of large size multimolecular micelles of 540 nm, although some low percentage of smaller micelles (85 nm), probably due to pristine polymer, could be also seen (Figure SI 20). Nile Red loading capacity and encapsulation efficiency were determined by fluorescence using a standard calibration line recorded in 90% DMF. The loading capacity values of Nile Red were 0.32 wt%, thus showing an efficiency of about 46 %, which is similar to the values described in the literature for PEG-*b*-PCL copolymers, containing also highly hydrophobic micellar cores [30]. Nile Red release was performed by mixing 2.0 mL of encapsulated material and 2.0 mL of a 3.0% H_2O_2, incubating at 37 ºC and measuring the fluorescence at determined times. Figure 4 shows the representation of the Nile Red fluorescence versus time in presence and absence of hydrogen peroxide.

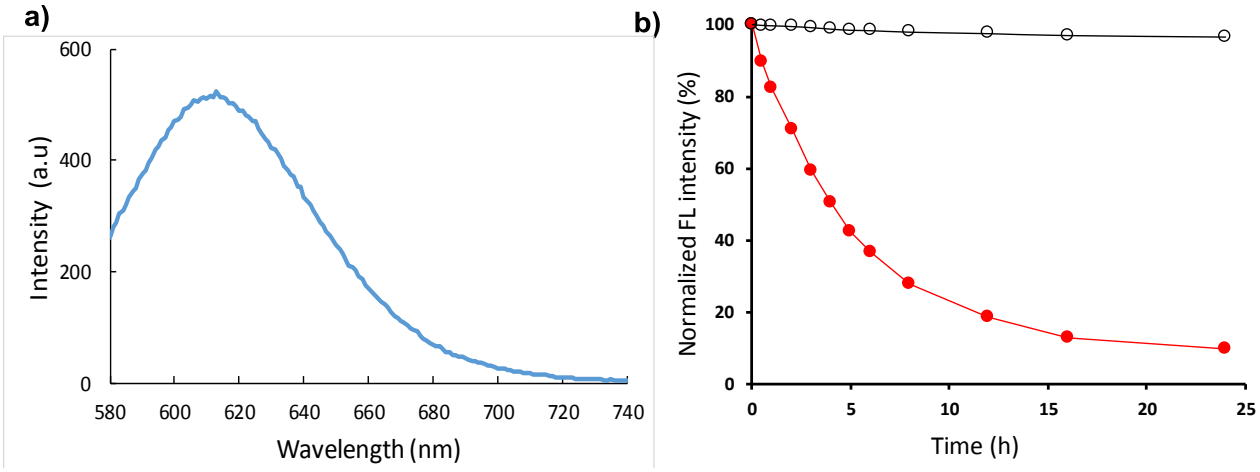

Figure 4. a) Fluorescent emission spectrum of Nile Red loaded $mPEG_{12}$-*b*-$PTHEA_{15}$ micelles (2 $mg.L^{-1}$). b) Nile Red fluorescence in micelles of $mPEG_{12}$-*b*-$PTHEA_{15}$ as a function of time in presence of 1.5 % (w/v) H_2O_2 (plain dots) and in absence of H_2O_2 (hollow dots).

As can be seen, only a slight fluorescence decrease is observed when the encapsulated material is in pure water. This could be due the multimolecular nature and the large size of the micelles that could retain some dye in the intermicellar interstices. On the contrary, in presence of H_2O_2, the fluorescence clearly decreases due to the progressive oxidation of the PTEHA moiety, the consequent destruction of the micellar container and the release of the insoluble Nile Red. Thus, even though the limited loading capacity, this thioether-containing systems could be used for some drug-release applications. Biocompatibility of these materials has not yet studied but similar systems based on poly(ethylene glycol)-b-poly(ω-thioether ester)'s showed no cytotoxicity [30]. Additionally, previous studies on 10-undecylenic acid-derived polymers showed also good biodegradability [51] and no cytotoxicity response [55].

CONCLUSIONS

Oxidation-responsive biodegradable amphiphilic block copolymers have been synthesized by CALB-catalyzed self-polycondensation of 11-((2-hydroxyethyl)thio)undecanoic acid (TEHA) initiated by methoxy polyethyleneglycol (mPEG-OH) of different lengths. Four different copolymers with similar composition to the feed have been obtained according to NMR characterization. Their oxidation behaviour in front of H_2O_2 under PTC conditions has been studied. Sulfone and sulfoxide groups in the structure of the oxidized products of both PTEHA and $mPEG_n$-*b*-$PTHEA_m$ have been identified using NMR, FTIR and Raman spectroscopies and no significant polymer degradation was observed.

The different block copolymers were able to self-assemble to form nanosized micelles in aqueous solution with low critical micelle concentration (0.16 to 0.51 mg/mL) showing potential application as responsive systems in drug delivery. Micellar characteristics investigated by dynamic light scattering (DLS) show the formation of monomodal multimolecular micellar assemblies of 220-250 nm in the case of $mPEG_{12}$ copolymers and a

bimodal distribution (with some higher aggregates) in the case of $mPEG_{45}$ copolyesters. TEM in drying mode however showed round shaped monomolecular micelles of 15-40 nm. Micelles of $mPEG_{12}$-*b*-$PTHEA_{15}$ were loaded with Nile red as model of hydrophobic drug, and were disassembled upon addition of H_2O_2. Efficient dye release within few hours was observed confirming the oxidation of hydrophobic cores and the dismantling of the micellar structure showing the potential of these new type of oxidation-responsive polymeric materials.

ACKNOWLEDGMENTS

The authors express their thanks to MICINN of Spain with Grants (MAT2014-53652-R) and (MAT2017-82669-R) for financial support for this work.

REFERENCES AND NOTES

[1] D. K. Schneiderman, M. A. Hillmyer, 50th Anniversary Perspective: There is a great future in sustainable polymers, Macromolecules 50 (2017) 3733-3749. https://doi.org/10.1021/acs.macromol.7b00293

[2] A. Gandini, T. M. Lacerda, A. J. F. Carvalho, T. Trovatti, The progress of polymers from renewable resources: furans, vegetable oils and polysaccharides, Chem. Rev. 116 (2016) 1637–1669. https://doi.org/10.1021/acs.chemrev.5b00264

[3] A. Gandini, T. M. Lacerda, From monomers to polymers from renewable resources: Recent advances. Prog. Polym. Sci. 48 (2015) 1-39. https://doi.org/10.1016/j.progpolymsci.2014.11.002

[4] Y. Zhu, C. Romain, C. K. Williams, Sustainable polymers from renewable resources, Nature 540 (2016) 354–362. https://doi.org/10.1038/nature21001

[5] S. Bigot, M. Daghrir, A. Mhanna, G. Boni, S. Pourchet, L. Lecamp, L. Plasseraud, Undecylenic acid: a tunable bio-based synthon for materials applications, Eur. Polym. J. 74 (2016) 26-37. https://doi.org/10.1016/j.eurpolymj.2015.11.008

[6] Z. Beyazkilic, G. Lligadas, J. C. Ronda, M. Galià, V. Cádiz, Vinylsulfide-containing polyesters and copolyesters from fatty acids: Thiol-yne monomer synthesis and thiol-ene functionalization, Macromol. Chem. Phys. 215 (2014) 2248-2259. https://doi.org/10.1002/macp.201400191

[7] Z. Beyazkilic, G. Lligadas, J. C. Ronda, M. Galià, V. Cádiz, Synthesis and functionalization of vinylsulfide and ketone-containing aliphatic copolyesters from fatty acids, Polymer 79 (2015) 290-298. https://doi.org/10.1016/j.polymer.2015.10.024

[8] C. Lluch, M. Calle, G. Lligadas, J. C. Ronda, M. Galià, V. Cádiz, Versatile post-polymerization modifications of a functional polyester from castor oil, Eur. Polym. J. 72 (2015) 64-71. https://doi.org/10.1016/j.eurpolymj.2015.09.005

[9] C. Valverde, G. Lligadas, J. C. Ronda, M. Galià, V. Cádiz, Hydroxyl functionalized renewable polyesters derived from 10-undecenoic acid: polymer structure and postpolymerization modification, Eur. Polym. J. 105 (2018) 68-78. https://doi.org/10.1016/j.eurpolymj.2018.05.026

[10] L. Ruíz, G. Lligadas, J.C. Ronda, M. Galià, V. Cadiz, Synthesis of acid degradable oxidation responsive poly(β-thioether ester)s from castor oil, Eur. Polym. J. 110 (2019) 183-191. https://doi.org/10.1016/j.eurpolymj.2018.11.026

[11] A. Kausar , S. Zulfiqar, M.I. Sarwar, Recent developments in sulfur-containing polymers, Polym. Rev. 54 (2014) 185-267. https://doi.org/10.1080/15583724.2013.863209

[12] S. Aksakal, R. Aksakal C. R. Becer, Thioester functional polymers, Polym. Chem. 9 (2018) 4507-4516. https://doi.org/10.1039/C8PY00872H

[13] Z. Sun, H. Huang, L. Li, L. Liu, Y. Chen, Polythioamides of high refractive index by direct polymerization of aliphatic primary diamines in the presence of elemental sulfur, Macromolecules 50 (2017) 8505-8511. https://doi.org/10.1021/acs.macromol.7b01788

[14] T. Tian, R. Hu, B. Z. Tang, Room temperature one-step conversion from elemental sulfur to functional polythioureas through catalyst-free multicomponent polymerizations, J. Am. Chem. Soc. 140 (2018) 6156–6163. https://doi.org/10.1021/jacs.8b02886

[15] M. Luo, Y. Li, Y-Y Zhang, X-H Zhang, Using carbon dioxide and its sulfur analogues as monomers in polymer synthesis, Polymer 82 (2016) 406-431. https://doi.org/10.1016/j.polymer.2015.11.011

[16] E. M. López-Vidal, G. L. Gregory, G. Kociok-Köhn, A. Buchard, Polymers from sugars and CS_2: synthesis and ring-opening polymerisation of sulfur-containing monomers derived from 2-deoxy-D-ribose and D-xylose, Polym. Chem. 9 (2018) 1577-1582. https://doi.org/10.1039/C8PY00119G

[17] I. Gomez, A. Fdz De Anastro, O. Leonet, J. A. Blazquez, H-J. Grande, J. Pyun, D. Mecerreyes, Sulfur polymers meet poly(ionic liquid)s: Bringing new properties to both polymer families, Macromol. Rapid Commun. 39 (2018) 1800529. https://doi.org/10.1002/marc.201800529

[18] M. A. C. Stuart, W. T. S. Huck, J. Genzer, M. Müller, C. Ober, M. Stamm, G. B. Sukhorukov, I. Szleifer, V. V. Tsukruk, M. Urban, F. Winnik, S. Zauscher, I. Luzinov, S. Minko, Emerging applications of stimuli-responsive polymer materials, Nat. Mater. 9 (2010) 101-113. https://doi.org/10.1038/nmat2614

[19] F. Seidi, R. Jenjob, D. Crespy, Designing smart polymer conjugates for controlled release of payloads Chem. Rev. 118 (2018) 3965-4036. https://doi.org/10.1021/acs.chemrev.8b00006

[20] L. Zhou, H. Wang, Y. Li, Stimuli-responsive nanomedicines for overcoming cancer multidrug resistance, Theranostics 8 (2018) 1059-1074. https://doi.org/10.7150/thno.22679

[21] M. Zhou, K. Wen, Y. Bi, H. Lu, J. Chen, Y. Hu, Z. Chai, The application of stimuli-responsive nanocarriers for targeted drug delivery, Curr. Top. Med. Chem. 17 (2017) 2319-2334. https://doi.org/10.2174/1568026617666170224121008

[22] H. Hatakeyama, Recent advances in endogenous and exogenous stimuli-responsive nanocarriers for drug delivery and therapeutics, Chem. Pharm. Bull. 65 (2017) 612-617. https://doi.org/10.1248/cpb.c17-00068

[23] M. S. Shim, Y. Xia, A reactive oxygen species (ROS)-responsive polymer for safe, efficient, and targeted gene delivery in cancer cells. Angew. Chem., Int. Ed. 52 (2013) 6926-6929. https://doi.org/10.1002/anie.201209633

[24] Y. Li, H. Bai, H. Wang, Y. Shen, G. Tang, Y. Ping, Reactive oxygen species (ROS)-responsive nanomedicine for RNAi-based cancer therapy, Nanoscale 10 (2018) 203-214. https://doi.org/10.1039/C7NR06689A

[25] G. Saravanakumar, J. Kim, W. J. Kim, Reactive-oxygen-species-responsive drug delivery systems: Promises and challenges. Adv. Sci. (Weinh) 4 (2017) 1600124. https://doi.org/10.1002/advs.201600124

[26] C.-C. Song, F.-S. Du, Z.-C. Li, Oxidation-responsive polymers for biomedical applications. J. Mater. Chem. B 2 (2014) 3413-3426. https://doi.org/10.1039/c3tb21725f

[27] L. Xu, M. Zhao, H. Zhang, W. Gao, Z. Guo, X. Zhang, J. Zhang, J. Cao, Y. Pu, B. He, Cinnamaldehyde-based poly(ester-thioacetal) to generate reactive oxygen species for fabricating reactive oxygen species-responsive nanoparticles, Biomacromolecules 19 (2018) 4658-4667. https://doi.org/10.1021/acs.biomac.8b01423

[28] M. K. Gupta, J. R. Martin, T. A. Werfel, T. W. Shen, J. M. Page, C. L. Duvall, Cell protective, ABC triblock polymer-based thermoresponsive hydrogels with ROS-triggered degradation and drug release, J. Am. Chem. Soc. 136 (2014) 14896-14902. https://doi.org/10.1021/ja507626y

[29] R. D'Arcy, A. Siani, E. Lallana, N. Tirelli, Influence of primary structure on responsiveness. Oxidative, thermal, and thermo-oxidative responses in polysulfides, Macromolecules, 48 (2015) 8108-8120. https://doi.org/10.1021/acs.macromol.5b02007

[30] W-X. Wu, X-L, Yang, B-Y. Liu, Q-F. Deng, M-M. Xun, N. Wang, X-Q Yu, Lipase-catalyzed synthesis of oxidation-responsive poly(ethylene glycol)-*b*-poly(β-thioether ester) amphiphilic block copolymers, RSC Adv. 6 (2016) 11870-11879. https://doi.org/10.1039/C5RA21779B

[31] J. Wang, D. Li, W.Tao, Y. Lu, X. Yang, J. Wang, Synthesis of an oxidation-sensitive polyphosphoester bearing thioether group for triggered drug release, Biomacromolecules 20 (2019) 1740-1747. https://doi.org/10.1021/acs.biomac.9b00101

[32] C. D. Vo, G. Kilcher, N. Tirelli, Polymers and sulfur: what are organic polysulfides good for? preparative strategies and biological applications, Macromol. Rapid Commun. 30 (2009) 299-315. https://doi.org/10.1002/marc.200800740

[33] J. Wang, X. Sun, W. Mao, W. Sun, J. Tang, M. Sui, Y. Shen, Z. Gu, Tumor redox heterogeneity-responsive prodrug nanocapsules for cancer chemotherapy, Adv. Mater. 25 (2013) 3670–3676. https://doi.org/10.1002/adma.201300929

[34] K. M. Poole, C. E. Nelson, R. V. Joshi, J. R. Martin, M. K. Gupta, S. C. Haws, T. E. Kavanaugh, M. C. Skala, C. L. Duvall, ROS-responsive microspheres for on demand antioxidant therapy in a model of diabetic peripheral arterial disease. Biomaterials 41 (2015) 166–175. https://doi.org/10.1016/j.biomaterials.2014.11.016

[35] H. Deng, X. Zhao, L. Deng, J. Liu, A. Dong, Reactive oxygen species activated nanoparticles with tumor acidity internalization for precise anticancer therapy. J. Control. Release 255 (2017) 142–153. https://doi.org/10.1016/j.jconrel.2017.04.002

[36] G. Gaucher, M-H. Dufresne, V. P. Sant, N. Kang, D. Maysinger, J-C. Leroux, Block copolymers micelles: preparation, characterization and application in drug delivery, J. Control. Release 109 (2010) 169-188. https://doi.org/10.1016/j.jconrel.2005.09.034

[37] I. N. Kurniasih, H. Liang, S. Kumar, A. Mohr, S.K. Sharma, J. P. Rabe, R. Haag, A bifunctional nanocarrier based on amphiphilic hyperbranched polyglycerol derivatives, J. Mat. Chem. B, 1 (2013) 3569-3577. https://doi.org/10.1039/C3TB20366B

[38] K. Kamenova, E. Haladjova, G. Grancharov, M. Kyulavska, V. Tzankova, D. Aluani, K. Yoncheva, S. Pispas, P. Petrov, Co-assembly of block copolymers as a tool for developing novel micellar carriers of

insulin for controlled drug delivery, Eur. Polym. J. 104 (2018) 1-9. https://doi.org/10.1016/j.eurpolymj.2018.04.039

[39] Y. Mai, A. Eisenberg, Self-assembly of block copolymers, Chem. Soc. Rev. 41 (2012) 5969-5985. https://doi.org/10.1039/C2CS35115C

[40] M. Cagel, F. C. Tesan, E. Bernabeu, M. J. Salgueiro, M. B. Zubillaga,, M. A. Moretton, D. A. Chiappetta, Polymeric mixed micelles as nanomedicines: achievements and perspectives, Eur. J. Pharm. Biopharm. 113 (2017) 211−228. https://doi.org/10.1016/j.ejpb.2016.12.019

[41] A.S. Deshmukh, P. N. Chauhan, M. N. Noolvi, K. Chaturvedi, K. Ganguly, S. S. Shukla, M. N. Nadagouda, T. M. Aminabhavi, Polymeric micelles: Basic research to clinical practice, Int. J. Pharm. 532 (2017) 249−268. https://doi.org/10.1016/j.ijpharm.2017.09.005

[42] N. Toncheva-Moncheva, P. Bakardzhiev, S. Rangelov, B. Trzebicka, A. Forys, P. D. Petrov, Linear amphiphilic polyglycidol/poly(ε-caprolactone) block copolymers prepared via "click"chemistry-based concept, Macromolecules 52 (2019) 3435-3447. https://doi.org/10.1021/acs.macromol.9b00366

[43] P. Tundo, G. P. Romanelli, PG. Vázquez, F. Aricò. Multiphase oxidation of alcohols and sulfides with hydrogen peroxide catalyzed by heteropolyacids. Cat. Commun. 11 (2010) 1181-1184. https://doi.org/10.1016/j.catcom.2010.06.015

[44] X. Fu, Y. Ma, Y. Shen, W. Fu and Z. Li. Oxidation-responsive PEGylated poly-L-cysteine and solution properties studies. Biomacromolecules 15 (2014) 1055-1061. https://doi.org/10.1021/bm5000554

[45] J. Aguiar, P. Carpena, J.A. Molina-Bolívar, C.C. Ruiz, On the determination of the critical micelle concentration by the pyrene 1:3 ratio method, J Colloid Interface Sci. 258 (2003) 116-122. https://doi.org/10.1016/S0021-9797(02)00082-6

[46] X. Ma, X. Huang, G. Huang, L. Li, Y. Wang, X. Luo, D. A. Boothman, J. Gao, Prodrug strategy to achieve lyophilizable, high drug loading micelle formulations through diester derivatives of β-Lapachone. Adv. Healthcare Mater. 3 (2014) 1210-1246. https://doi.org/10.1002/adhm.201300590

[47] C. Valverde; G. Lligadas; J.C. Ronda; M. Galià, V. Cádiz. PEG-modified poly(10,11-dihydroxyundecanoic acid) amphiphilic copolymers. Grafting versus macromonomer copolymerization approaches using CALB, Eur. Polym. J. 109 (2018) 179-190. https://doi.org/10.1016/j.eurpolymj.2018.09.032

[48] A. Mahapatro, A. Kumar, R.A. Gross, Mild, solvent-free ω-hydroxyacid polycondensations by Candida antarctica Lipase B, Biomacromolecules 5 (2004) 62-68. https://doi.org/10.1021/bm0342382

[49] H. Ebata, K. Toshima, S. Matsumura, Lipase-catalyzed synthesis and curing of high-molecular-weight polyricinoleate, Macromol. Biosci. 7 (2007) 798-803. https://doi.org/10.1002/mabi.200700018

[50] Z. Beyazkilic, G. Lligadas, J.C. Ronda, M. Galià, V. Cádiz. Fully biobased triblock copolyesters from l-Lactide and sulfur containing castor oil derivatives: Preparation, oxidation and characterization, Polymer 68 (2015) 101-110. https://doi.org/10.1016/j.polymer.2015.05.013

[51] C. Valverde, G. Lligadas, J. C. Ronda, M. Galià, V. Cádiz, Hydrolytic degradation studies of aliphatic 10-undecenoic acid-based polyesters, Polym. Degrad. Stab. 155 (2018) 84-94. https://doi.org/10.1016/j.polymdegradstab.2018.07.012

[52] A. Khan, S.K. Sharma, A. Kumar, A.C. Watterson, J. Kumar, V.S. Parmar, Novozym 435-catalyzed syntheses of polyesters and polyamides of medicinal and industrial relevance, ChemSusChem 7 (2014) 379-390. https://doi.org/10.1002/cssc.201300343

[53] M. Kumari, A. K. Singh, S. Kumar, K. Achazi, S. Gupta, R. Haag, S. K. Sharma, Synthesis of amphiphilic dendronized polymers to study their self-assembly and transport behaviour, Polym. Avd. Technol. 25 (2014) 1208-1215. https://doi.org/10.1002/pat.3293

[54] G.B. Ray, I. Charkraborty, S.P. Moulik, Pyrene absorption can be a convenient method for probing critical micellar concentration (cmc) and indexing micellar polarity, J. Colloid Interface Sci. 294 (2006) 248-254. https://doi.org/10.1016/j.jcis.2005.07.006

[55] R. Gonzalez-Paz, C. Lluch, G. Lligadas, J.C. Ronda, M. Galià, V. Cádiz, A green approach toward oleic- and undecylenic acid-derived polyurethanes, J. Polym. Sci. Part A. Polym. Chem. 49 (2011) 2407-2416. https://doi.org/10.1002/pola.24671

GRAPHICAL ABSTRACT